

## The Origin of the Distorted Close-Packed Elemental Structure of Indium\*\*

Ulrich Häussermann,\* Sergei I. Simak, Rajeev Ahuja, Börje Johansson, and Sven Lidin

The unique structure of indium belongs to a small group of metallic structures that deviate from the close-packed trend usually displayed by metallic elements. Its body-centered tetragonal (bct) unit cell, with lattice parameters  $a = 3.2525$  and  $c = 4.9465$  Å,<sup>[1]</sup> contains the two equivalent atoms at the corners and the center of the cell. The structure is easily visualized as a slightly distorted close packed cubic (fcc) structure with a  $c/a$  ratio of 1.5208 (Figure 1), compared to  $\sqrt{2}$  for ideal fcc. Thus the environment of the 12 nearest neighbors in the fcc structure is split into two sets separated by distances  $d_1$  and  $d_2$ , as indicated in Figure 1.

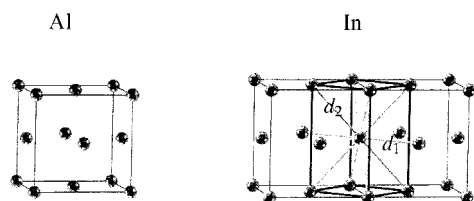


Figure 1. The structure of tetragonal In compared to the close-packed fcc structure of Al.

Why does In adopt this more open-packed structure of lower symmetry, whereas the lighter homologue Al crystallizes in the highly symmetric fcc structure? In the early 1970s Heine and Weaire<sup>[2]</sup> and later Hafner and Heine<sup>[3]</sup> addressed this question in the context of a beautiful work, where they related the crystal structures of the elements on the common ground of pseudopotential theory. For In it was found that the changes in the size of the ionic core, compared to that of Al, are responsible for the instability of the fcc structure. However, the pseudopotential results are rather qualitative, and the success of this theory is astonishing in the case of In because—as we will see later—the stabilizing energy which In gains by distortion of the fcc structure is extremely small.

The systematic exploration of the electronic reasons behind the “unusual”, low-symmetry metal structures is highly challenging, and reliable quantitative results have not been accessible until recently with the advent of high-accuracy full-

potential techniques in the framework of density functional theory.<sup>[4]</sup> Here we treat the question of the origin of the low-symmetry In structure and the high-symmetry Al structure on such a quantitative ground by means of ab initio full-potential calculations (see the computational methods) and relate the results to the differences in the atomic properties of these two elements.

We started our investigation by calculating the change in the total energy of Al and In upon altering the  $c/a$  ratio from the ideal value of  $\sqrt{2}$  for the fcc structure to lower and higher values, while keeping the volume constant and equal to the experimental ground-state volumes of the elements. Figure 2 depicts the results. For Al, where the fcc structure is the

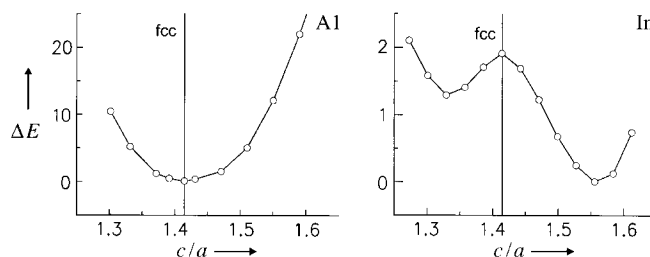


Figure 2. Variations in total energy (in meV per atom) as a function of  $c/a$  at the respective experimental ground-state volumes  $V_0$  for Al and In. Note the different energy scales.

ground-state structure, the tetragonal distortion leads to a parabolic change in total energy with respect to  $c/a$ , where the minimum of the curve corresponds to the  $c/a$  ratio of the fcc structure. For In, however, a very remarkable result is obtained: The total energy curve exhibits a double-well behavior with two minima and a local maximum exactly at a  $c/a$  ratio corresponding to the ideal fcc structure. This behavior is reminiscent of a Peierls distortion in solids or a Jahn–Teller distortion in molecular compounds. The deeper minimum at a  $c/a$  ratio of 1.55 (at 0 K) is in agreement with the observed ground-state structure of In and compares very well with the experimental value of 1.521 (at 298 K). The stabilizing energy of the ground-state structure with respect to the fcc structure turns out to be extremely small. It is below 2 meV per atom, which corresponds to a temperature of about 20 K. The stabilization of the possible metastable In structure with a  $c/a$  ratio of approximately 1.33 is only one-third of this value. Thus the energy changes observed along the tetragonal distortion path are an order of magnitude smaller for In than for Al.

In this context, it is instructive to divide the total energy into the band energy, which represents the sum over the occupied states and thus is most transparent from a chemical point of view, and a part consisting of the remaining contributions (the electrostatic interaction and the exchange–correlation energy). Figure 3 shows the result of this partition. In both cases the trend in the changes of the band energy coincides with that of the total energy: For Al we find a relative minimum and for In a relative maximum at a  $c/a$  ratio of  $\sqrt{2}$ . The sum of the remaining parts of the total energy displays exactly the opposite tendency, favoring a distorted structure for Al and the

[\*] Dr. U. Häussermann, Prof. S. Lidin  
Department of Inorganic Chemistry  
Stockholm University  
S-10691 Stockholm (Sweden)  
Fax: (+46)8-152187  
E-mail: ulrich@inorg.su.se

Dr. S. I. Simak  
Department of Applied Physics  
Chalmers University of Technology and Göteborg University  
S-41296 Gothenburg (Sweden)  
Dr. R. Ahuja, Prof. B. Johansson  
Condensed Matter Theory Group, Physics Department  
Uppsala University  
S-75121 Uppsala (Sweden)

[\*\*] This work was supported by the Swedish National Science Research Council (NFR) and the Göran Gustafsson Foundation.

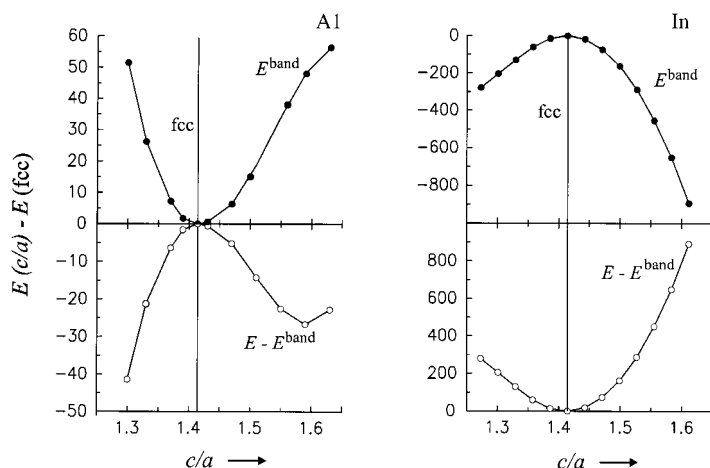


Figure 3. Partition of the total energy (in meV per atom) into the band energy term  $E^{\text{band}}$  (closed circles) and the sum of the remaining contributions  $E - E^{\text{band}}$  (open circles) as a function of  $c/a$  at the respective experimental ground-state volumes  $V_0$  for Al and In.

high-symmetry fcc structure for In. Thus, we may identify the band-energy term as the leading contribution to the stability of the ground-state structures of Al and In. How can we explain the opposite changes in the band energies of Al and In when deforming their crystal structure from a high-symmetry close-packed to a more open-packed atomic arrangement?

Aluminum and indium belong to the triel elements (Group 13), which represent the border between the elements with exclusively close-packed structures that show metal bonding and the tetrel elements (Group 14) crystallizing in the diamond structure that show covalent bonding. Indeed, the two most electronegative representatives of the triels, boron and gallium, exhibit ground-state structures with large covalent bonding contributions. Naturally, as the number of valence electrons increases and the separation of the atomic s and p levels decreases when going from the alkali metals to the tetrels, mixing of the s and p bands becomes a more and more significant ingredient in the bonding for the elemental structures. The s–p mixing is first recognized in the semi-metallic behavior of the alkaline earth metals Ca and Sr, and leads finally to the opening of a band gap at the Fermi level for the tetrel elements.<sup>[6]</sup> Interestingly, we find that the ratio between the total number of p and s states ( $N_p/N_s$ ) calculated inside the muffin-tin spheres of Al and In as a function of  $c/a$  (Figure 4) displays a trend that is the reverse of that for the corresponding band energies (Figure 3): The  $N_p/N_s$  ratio gains

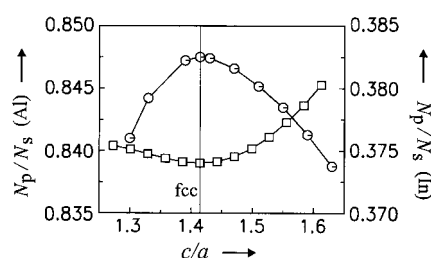


Figure 4. Changes of the ratio of the number of p and s states in the muffin-tin spheres ( $N_p/N_s$ ) as a function of  $c/a$  for Al (circles) and In (squares) at the respective experimental ground-state volumes.

a maximum value for Al and a minimum value for In at  $c/a = \sqrt{2}$ . Consequently, the apparent tendency for Al and In is to adopt a ground-state structure where s–p mixing is either maximal (Al) or increased by distortion (In). This finding fits nicely to our recent investigation of the stability of  $\alpha$ -Ga with respect to other structural alternatives. There we also obtained a maximum in the ratio  $N_p/N_s$  for the most stable geometry, which corresponds to the experimental  $\alpha$ -Ga structure, and related this result with a situation of “maximum covalency” in  $\alpha$ -Ga.<sup>[7]</sup>

The analysis of the orbital character of the band structures for fcc-Al and fcc-In (at their experimental ground-state volumes) reveals the reason behind the different distortion behavior of In and Al (Figure 5).<sup>[8]</sup> For Al small local band gaps

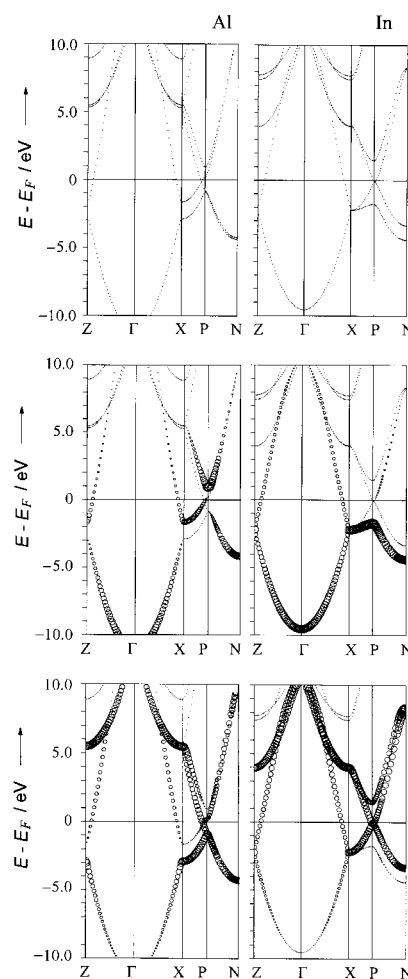


Figure 5. Band structures (top) for fcc-Al and fcc-In at the respective experimental ground-state volumes<sup>[8]</sup> as well as the s (middle) and p character of the bands (bottom). The orbital character is proportional to the size of the circles used in the plots.

occur at the high-symmetry k points, which are a consequence of the mixing of the upwards running s band with a downwards running p band. The interaction between s and p bands is especially large along the direction  $N \rightarrow P$ , resulting in a band gap at P exactly at the Fermi level. In contrast to Al, s–p mixing in In is too weak for opening of local band gaps at the high-symmetry k points. Of course these differences are also reflected in the density of states (Figure 6). At low energies

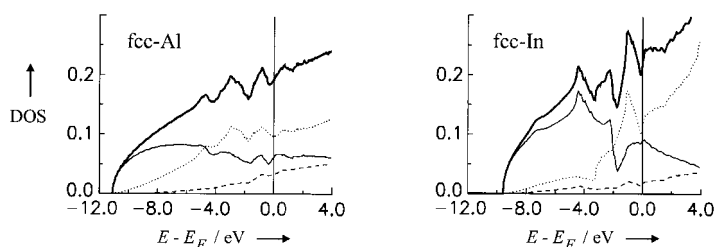


Figure 6. Total density of states (DOS; bold lines) together with the s (solid lines), p (dotted lines), and d orbital contributions (dashed lines) of fcc-Al and fcc-In at their respective experimental ground-state volumes. The unit for the total DOS is the number of electrons per eV.

the density of states shows a parabolic, free-electron-like distribution for both metals. In the case of Al at higher energies additional structuring is seen which is caused by the small band gaps at the high-symmetry points. For In the separation between the 5s and 5p bands is expressed by a spikey behavior with a large p contribution just below the Fermi level, whereas for Al the s and p contribution to the density of states appear much more homogeneously distributed.

The opposite dispersion of the s and p bands along certain symmetry lines is due to the difference in parity of the orbitals. The bands might cross if the size of the s–p separation at the atomic levels is not too large and/or the size of the dispersion of the bands under consideration is sufficiently pronounced.<sup>[9]</sup> The energies of the p valence orbitals are almost identical ( $\epsilon_{3p}(\text{Al}) = -5.984$ ,  $\epsilon_{5p}(\text{In}) = -5.785$  eV<sup>[10]</sup>), but the In 5s orbital is comparatively lower in energy ( $\epsilon_{5s}(\text{In}) = -10.122$  eV) than the Al 3s orbital ( $\epsilon_{3s}(\text{Al}) = -9.582$ ). The dispersion of the bands is essentially determined by the size of the overlap between the atomic orbitals, which itself is a function of the size of the atomic orbitals in relation to the distance between the atoms. The expectation values of the valence orbitals are  $\langle r \rangle_{3s} = 1.37$  and  $\langle r \rangle_{3p} = 1.82$  Å for Al, and  $\langle r \rangle_{5s} = 1.44$  and  $\langle r \rangle_{5p} = 1.99$  Å for In.<sup>[11]</sup> When taking into account the nearest neighbor distances in fcc-Al and fcc-In at the experimental ground-state volumes ( $d_{\text{NN}}(\text{Al}) = 2.86$ ,  $d_{\text{NN}}(\text{In}) = 3.33$  Å), it becomes immediately evident that especially the s–s overlap is considerably smaller in In. This leads to a much smaller dispersion of the s band compared to the situation for Al. These two factors, the lower lying s valence orbital energy and the smaller dispersion of the s band, prevent substantial s–p mixing for In in the fcc structure.

The stabilizing nature of s–p mixing was investigated by Burdett<sup>[9]</sup> on a model system consisting of a one-dimensional chain of atoms with an s and an appropriate p orbital. The result is summarized schematically in Figure 7. With strong s–p mixing (hybridization), the top of the lower band drops in energy and alters its exclusively s–s antibonding character into a p–p bonding one, while the upper band becomes completely antibonding. Thus the one-dimensional chain is maximally stabilized with an electron count corresponding to a completely filled lower band.

This simple picture is of great importance for the understanding of the structural stability of the metallic triels when assuming the band energy to be the structure-determining factor, and thus bonding is largely influenced by the low-lying s valence band. Imagine a close-packed arrangement with

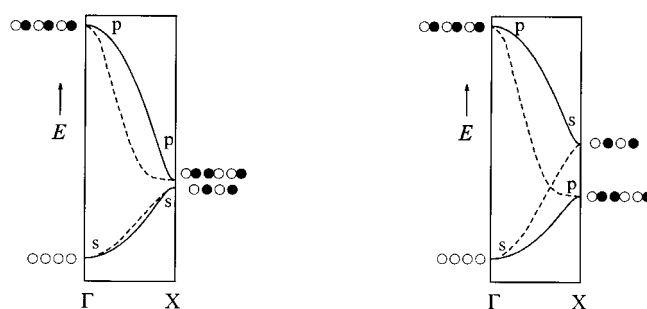


Figure 7. Schematic band structure for a linear chain of atoms with an s and a p orbital only for strong s–p mixing (right) and weak s–p mixing (left; based on ref. [9]). The dashed lines approximate the dispersion of the unhybridized bands. The appropriate orbital combinations at the high-symmetry k points are indicated.

unhybridized bands. Then for many directions in the Brillouin zone the electron count of these elements will produce a completely occupied s valence band with a large antibonding contribution (at the top of the band). This bonding situation is not especially favorable, and instead the triels try to obtain a structure where s–s antibonding states are raised above the Fermi level for the largest possible part of the Brillouin zone, or equivalently where the number of p states below the Fermi level is maximized (i.e., the ratio  $N_p/N_s$  is maximal). Aluminum condenses at a volume where strong s–p mixing is possible for the fcc structure, and, even more, is maximal for the close-packed arrangement with respect to the tetragonal distortion. Indium, however, condenses at a volume where s–p mixing is relatively weak. A distortion to a low-symmetry structure can now improve this situation, as some atoms move closer to each other and thus increase the interaction between s and p bands. This hypothesis is corroborated by a computer experiment performed by us, where we expanded Al to a volume of about  $V/V_0 = 1.3$ . At this volume s–p mixing is considerably suppressed for the fcc structure because the dispersion of the bands is diminished. To improve its bonding situation and take advantage of hybridized bands, Al could be expected to distort to a structure of lower symmetry. Indeed, we found the  $\alpha$ -Ga structure to be more stable at this expanded volume than the fcc structure.<sup>[12]</sup>

## Computational Methods

We calculated the change in the total energy of Al and In along the tetragonal distortion path of the fcc structure at constant volume (experimental ground-state volume  $V_0(\text{Al}) = 16.617$ ,  $V_0(\text{In}) = 26.164$  Å<sup>3</sup> per atom), and compared the results of the (scalar relativistic) full-potential linearized augmented plane wave (FLAPW) method<sup>[5a]</sup> with those of the (scalar relativistic) full-potential linear muffin-tin orbital (FP-LMTO) method.<sup>[5b]</sup> In full-potential techniques within the local-density approximation basis functions, electron densities, and potentials are calculated without any shape approximation.

In the case of the FLAPW calculations, a cut-off parameter  $R_{\text{m}}K_{\text{max}} = 10.0$  was used, yielding about 250 plane waves for In and 170 for Al. For Al a [Ne] configuration was considered as the core state, whereas for In the [Kr] configuration was used and the 4d states were treated as local orbitals. The exchange–correlation potential was parametrized according to Perdew and Wang.<sup>[5c]</sup> The reciprocal space integrations in the irreducible tetragonal Brillouin zone (BZ) were performed with the tetrahedron method.

In the case of the FP-LMTO calculations, we made use of valence band s, p, and d basis functions for both Al and In. For In pseudocore 4d states were included in the basis as well; that is, the resulting basis always formed a single, fully hybridizing basis set. The exchange–correlation potential was parametrized according to Hedin and Lundqvist.<sup>[5d]</sup> For sampling the irreducible wedge of the BZ we used the special k points with a Gaussian smearing of width 20 mRy.

To ensure convergency several standard tests were performed for both methods, such as increasing the number of k points used in the summation over the BZ. The calculated energy differences ( $E_{\text{c/a}} - E_{\text{fcc}}$ ) and band structures were found to be virtually identical for the two full-potential techniques. The presented energy differences and density of states were obtained from FP-LMTO calculations, the presented band structures from FLAPW calculations.

Received: January 18, 1999 [Z12929IE]  
German version: *Angew. Chem.* **1999**, *111*, 2155–2159

**Keywords:** ab initio calculations • aluminum • bond theory • elemental structures • indium

- [1] J. Donohue, *The Structure of the Elements*, Wiley, New York, **1974**.
- [2] V. Heine, D. Weaire, *Solid State Phys.* **1970**, *24*, 249.
- [3] J. Hafner, V. Heine, *J. Phys. F* **1983**, *13*, 2479.
- [4] P. Söderlind, O. Eriksson, B. Johansson, J. M. Wills, A. M. Boring, *Nature (London)* **1995**, *374*, 524; R. Ahuja, O. Eriksson, J. M. Wills, B. Johansson, *Phys. Rev. Lett.* **1995**, *75*, 280; S. I. Simak, U. Häussermann, I. A. Abrikosov, O. Eriksson, J. M. Wills, S. Lidin, B. Johansson, *Phys. Rev. Lett.* **1997**, *79*, 1333.
- [5] a) Program package WIEN97: P. Blaha, K. Schwarz, J. Luitz, *Program WIEN97: A Full Potential Linearized Augmented Plane Wave Package for Calculating Crystal Properties* (K. Schwarz, Vienna University of Technology, Austria), **1999** (ISBN 3-9501031-0-4); b) J. M. Wills, unpublished results; J. M. Wills, B. R. Cooper, *Phys. Rev. B* **1987**, *36*, 3809; c) J. P. Perdew, Y. Wang, *Phys. Rev. B* **1992**, *45*, 13244; d) L. Hedin, B. I. Lundqvist, *J. Phys. C* **1971**, *4*, 2064.
- [6] D. G. Pettifor, *Bonding and Structure of Molecules and Solids*, Clarendon Press, Oxford, **1995**.
- [7] U. Häussermann, S. I. Simak, I. A. Abrikosov, S. Lidin, *Chem. Eur. J.* **1997**, *3*, 904.
- [8] For the calculation of the band structures we used a tetragonal body centered (bct) unit cell with the appropriate  $c/a$  ratio of  $\sqrt{2}$ . Thus, the two different nearest neighbor distances  $d_1$  and  $d_2$  (Figure 1) are both equal to the lattice constant  $a$ , and in reciprocal space the two directions  $\Gamma$ -Z and  $\Gamma$ -X become degenerate (Figure 5).
- [9] J. K. Burdett, *Chemical Bonding in Solids*, Oxford University Press, Oxford, **1995**.
- [10] C. E. Moore, *Atomic Energy Levels*, National Bureau of Standards, Washington, DC, **1949**.  $\epsilon_p$  was taken as the negative experimental ionization energy from the corresponding p orbital;  $\epsilon_s$  was calculated as  $\epsilon_p$  minus the lowest s  $\rightarrow$  p excitation energy yielding the same spin multiplicity.
- [11] J. P. Desclaux, *At. Data Nucl. Data Tables* **1973**, *12*, 311.
- [12] R. Ahuja, S. I. Simak, unpublished results.

## Design and Development of the First Peptide-Chelating Bisphosphane Bioconjugate from a Novel Functionalized Phosphorus(III) Hydride Synthon\*\*

Hariprasad Gali, Srinivasa R. Karra,  
V. Sreenivasa Reddy, and Kattesh V. Katti\*

*Dedicated to Professor S. S. Krishnamurthy  
on the occasion of his 60th birthday*

The incorporation of metal-chelating units into peptide backbones (and related biomolecules) has become an area of intense interest because of the potential applications to catalysis<sup>[1]</sup> and biomedicine.<sup>[2]</sup> Among various ligands available, phosphanes are unique because they display versatile coordination chemistry with transition metals.<sup>[3]</sup> The secondary and tertiary structures of peptides to which they are attached may subsequently help in controlling the reactivity of phosphane-coordinated transition metals. Specifically, the chirality and related important stereospecific characteristics associated with biomolecules (e.g. peptides or proteins) may be transferred to the transition metals if peptides are immobilized with chelating units that are capable of coordinating with transition metals.<sup>[4]</sup> This approach of conjugating catalytically active transition metals to chiral biomolecules provides a straightforward route to chiral compounds with potential applications in enantioselective catalysis.<sup>[4]</sup> The incorporation of phosphanes into peptides (and proteins) will also help to engineer metal binding sites, which may eventually provide conformational integrity, biospecificity, and enhanced enzymatic activities.<sup>[5]</sup>

Bioconjugation of cytotoxic transition metals to receptor-active peptides may eventually provide effective vehicles for delivering cytotoxic moieties to specific tumors through receptor-mediated agonist or antagonist interactions.<sup>[6]</sup> In this context, peptides (or receptor-binding biomolecules) containing phosphane substituents are important in the design and development of tumor-specific radiopharmaceuticals.<sup>[7, 8]</sup> Despite significant catalytic and biomedical applications offered by such peptides (and proteins), synthetic strategies for producing such bioconjugates are still in their infancy. The elegant work by Gilbertson and co-workers on the incorporation of aryl- and cyclohexylphosphanes into specific peptides has provided impetus to this potentially burgeoning field of chemical and biomedical sciences.<sup>[9]</sup>

As part of our ongoing research on the development of functionalized phosphanes for biomedical and catalytic ap-

[\*] Prof. Dr. K. V. Katti, H. Gali, Dr. S. R. Karra, Dr. V. S. Reddy  
Department of Radiology  
Center for Radiological Research  
Allton Building Laboratories, Room 106  
University of Missouri-Columbia  
Columbia, MO 65211 (USA)  
Fax: (+1) 573-884-5679  
E-mail: kattik@missouri.edu

[\*\*] We thank Professor Wynn A. Volkert for valuable scientific input and support. This work was supported by DuPont Pharmaceuticals, USA, and the US Department of Energy.



Supporting information for this article is available on the WWW under <http://www.wiley-vch.de/home/angewandte/> or from the author.